Sharp

BNWL-817

3760 Bldg.

[redacted]

AN IN SITU WELD DEFECT DETECTOR ACOUSTIC EMISSION

W. D. JOLLY

SEPTEMBER 1968

[redacted]

AEC RESEARCH & DEVELOPMENT REPORT

BATTELLE NORTHWEST
BATTELLE MEMORIAL INSTITUTE PACIFIC NORTHWEST LABORATORY
BATTELLE BOULEVARD, P. O. BOX 999, RICHLAND, WASHINGTON 99352

BNWL-817

LEGAL NOTICE

PACIFIC NORTHWEST LABORATORY
RICHLAND, WASHINGTON
operated by
BATTELLE MEMORIAL INSTITUTE
for the
UNITED STATES ATOMIC ENERGY COMMISSION UNDER CONTRACT AT(45-1)-1830

PRINTED BY/FOR THE U. S. ATOMIC ENERGY COMMISSION

AEC-RL RICHLAND, WASH

BNWL-817

UC-23, Isotopes—Industrial Technology

AN IN SITU WELD DEFECT DETECTOR ACOUSTIC EMISSION

By

W. D. Jolly

Nondestructive Testing Department
Systems and Electronics Division

September 1968

BATTELLE MEMORIAL INSTITUTE
PACIFIC NORTHWEST LABORATORY
RICHLAND, WASHINGTON

Printed in the United States of America
Available from
Clearinghouse for Federal Scientific and Technical Information
National Bureau of Standards, U.S. Department of Commerce
Springfield, Virginia 22151
Price: Printed Copy $3.00; Microfiche $0.65

AN IN SITU WELD DEFECT DETECTOR ACOUSTIC EMISSION

W. D. Jolly

ABSTRACT

This report describes an investigation of the application of acoustic emission to the detection of weld defects during and immediately following the welding operation. Both manual and machine welds fabricated by the gas tungsten-arc process produce acoustic emission. Acoustic emission from welds in 304L and 316 SS is examined in detail. A correlation is made between acoustic emission rate and radiographic analysis data. A relationship between acoustic emission rate and weld defect region temperature is demonstrated. Acoustic emission pulse characteristics and spectral power distribution are presented. Problems involved in locating weld defects by means of acoustic emission signals are discussed.

TABLE OF CONTENTS

ABSTRACT	iii
LIST OF FIGURES	vii
INTRODUCTION	1
SUMMARY	1
ACOUSTIC EMISSION	2
EXPERIMENTAL RESULTS	3
ACOUSTIC EMISSION RATE	7
TEMPERATURE DEPENDENCE	10
VELOCITY MEASUREMENT	10
PULSE CHARACTERISTICS	14
EXPERIMENTAL EQUIPMENT	18
ACKNOWLEDGEMENTS	20
REFERENCES	20
APPENDIX	A-1
DISTRIBUTION	Distr-1

LIST OF FIGURES

1. Acoustic Emission from Single Pass Welds in 304L SS with Radiographs of Induced Defects 4

2. Comparison of Acoustic Emission from a Good Weld (A) and a Defective Weld (B) in 1/2 in. Stainless Steel Plate 6

3. Specimens Used for the Evaluation of Acoustic Emission from Welds 8

4. Acoustic Emission Rate from Single Pass Welds Relative to Defect Location 9

5. Weldment Temperature as a Function of Time from the Molten State 11

6. Acoustic Emission Rate as a Function of Defect Temperature (Average of 4 Induced Defects) 11

7. Measurement of Acoustic Emission Velocity 13

8. Acoustic Emission Pulses Which Demonstrate the Effect of Source Location on Pulse Shape 15

9. Spectral Power Distribution from a Single Acoustic Emission Pulse - 1 kHz to 320 kHz 17

10. Acoustic Emission Monitoring System 19

AN IN SITU WELD DEFECT DETECTOR ACOUSTIC EMISSION

W. D. Jolly

INTRODUCTION

Acoustic emission has been investigated as a candidate for an in situ nondestructive test for welds. Nondestructive methods for inspecting welds, such as radiography or ultrasonic techniques, are normally applied only after a weld is completed. An inspection method which indicates the occurrence of defects in a weld could provide immediate information to the welder. This would result in improved welding techniques, reduced rework time, and reduced fabrication costs. The work reported here was conducted to establish the feasibility of detecting the occurrence of weld defects by monitoring acoustic emission pulses resulting from the formation of defects.

SUMMARY

Acoustic emission was observed from a series of welds in stainless steel plate. A direct correlation was established between acoustic emission rate and radiographic analysis of single pass machine welds in 1/8 in. 304L SS plate containing induced defects at specific locations. We found that the onset of acoustic emission is delayed 20 to 45 sec as the defect region begins to cool; also that acoustic emission rate from induced defect regions increases as the defect region cools, reaching a peak at about 400 °C. Acoustic emission rate from multipass welds in 1/2 in. 304L and 316 SS plate was greater than the emission rate from the single pass welds by about an order of magnitude, and the same direct correlation between radiographic analysis and acoustic emission rate was found.

The apparent propagation velocity of the acoustic pulses from the induced defect regions varied as much as a factor of 2. This is interpreted to mean that the acoustic emission signals

reach the receivers by indirect routes. The characteristic emission pulse shape and spectral distribution vary with distance or direction from the acoustic emission source. Since pulse lengths are sufficient to set up complex reflection patterns in the plate, the received signals are modified by multipath interference at the receiver location. Thus, the received signal characteristics are determined by source location, receiver location, and plate geometry.

The ability to detect certain types of weld defects by acoustic emission monitoring has been established. The primary advantage of this technique is that defects can be detected during the welding process. Acoustic emission techniques appear to be sensitive to microfissures beyond the resolution limits of presently applied ultrasonic and radiographic methods. Used in conjunction with other weld inspection methods, this technique could reduce significantly the rejection rate in final inspection of welds.

ACOUSTIC EMISSION

Research into the application of acoustic emission as a nondestructive tool has been directed primarily to the prediction of failure in structures under stress, such as reactor pressure vessels[1,2] or aircraft structural members.[3] Acoustic emission refers to the pressure wave which results from the release of energy in a material by deformation or fracture. Two types of acoustic emission signals have been identified: a repetative, low amplitude emission which increases in intensity with increasing stress and stress rate, and a pulse type signal which increases in repetition rate with increasing stress and stress rate.[1] A flaw in a material under load causes stress concentrations, which in turn cause a localized increase in acoustic emission pulse rate.

The heat affected zone of a weld satisfies all the conditions necessary to produce acoustic emission. During and following the welding operation, stress caused by thermal gradients can be sufficient to cause plastic deformation of the material, as well as cracking in the weld metal or along the fusion line.[4] Weld flaws such as inclusions, porosity, incomplete fusion, and crack formation should cause the acoustic emission to increase because of the high stress gradients which surround flaws.

EXPERIMENTAL RESULTS

Acoustic emission from three single pass, gas tungsten-arc, machine welds in 304L SS plate is shown in Figure 1. The data shown are acoustic emission pulses in a frequency band of 50 kHz to 300 kHz which exceed a threshold preset to exclude background noise and continuous acoustic emission signals resulting from deformation. The pulses have been rectified and integrated so that the vertical scale represents relative acoustic energy. The horizontal scale represents time (2 min/in.) from the start of the weld. The weld rate was 4 7/16 in/min. The radiographs show defects which consist largely of cracks induced by the addition of small amounts of titanium to the weldment. The radiographs are located above the acoustic emission resulting from each defect. A marker indicates the time at which the defect region was welded. The time delay between welding and the onset of acoustic emission is clearly visible. As expected, acoustic emission was present throughout the welds, but radiographic analysis showed defects only in the regions indicated. The low level acoustic emission pulses are believed to be the result of microfissures which normally occur in this weld configuration but are too small to show on the radiograph. The two defects in Weld 3 (C) and the second defect in Weld 2 (B) show as single large cracks in the

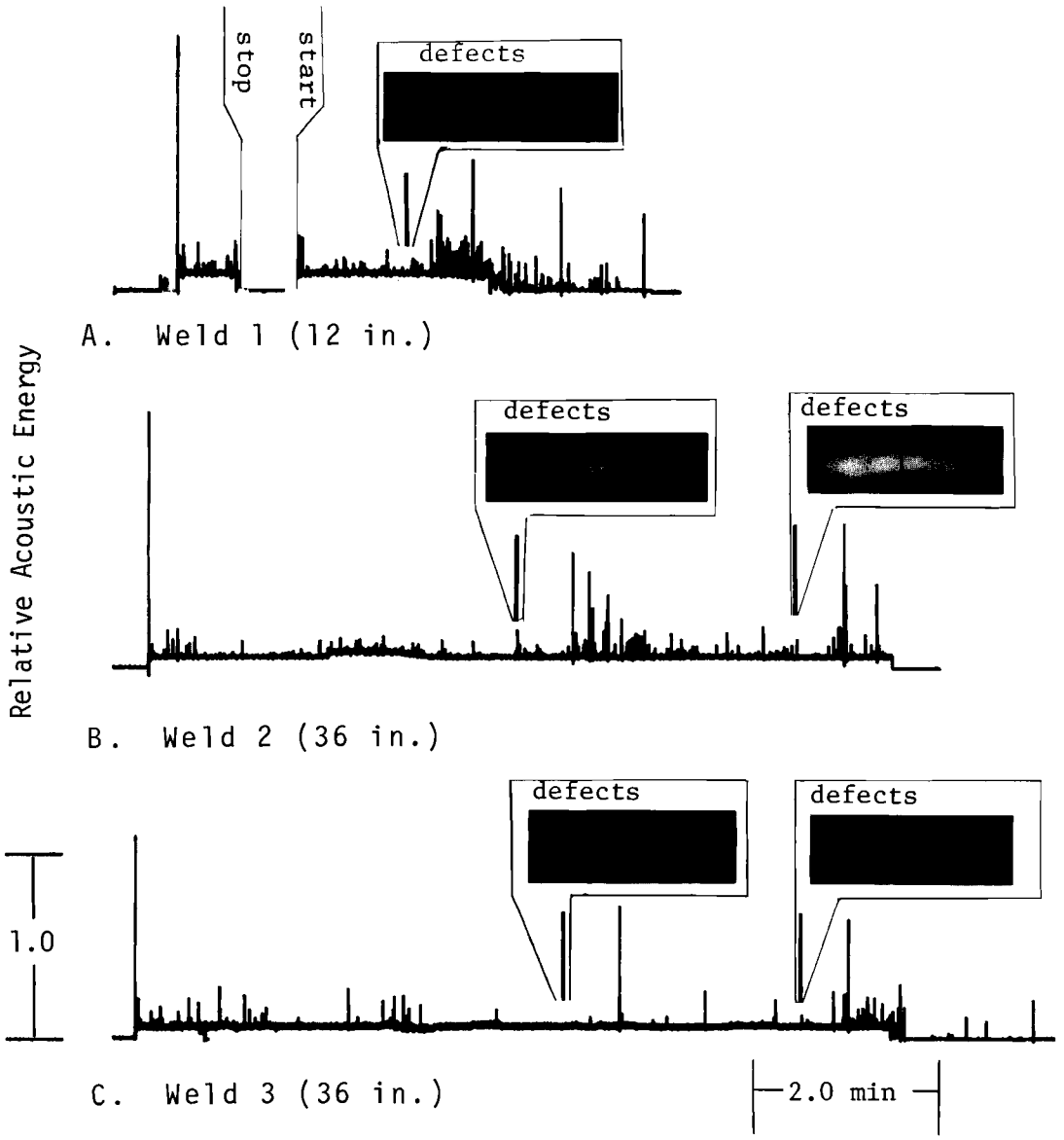

FIGURE 1. Acoustic Emission from Single Pass Welds in 304L SS with Radiographs of Induced Defects

radiographs, but the acoustic emission pulses indicate that these cracks developed in steps. Acoustic emission density from the defect in Weld 1 and the first defect in Weld 2 indicates the presence of microcracks.

Two manual, multipass, gas tungsten-arc welds made in 1/2 in. 304L and 316 SS are shown in Figure 2. (Note: The vertical scale of Figure 2 is reduced by a factor of 2 relative to Figure 1; the horizontal bars beneath each graph indicate successive weld passes separated by periods of cooling.) The acoustic energy and emission rate in both the good weld (A) and the defective weld (B) are noticeably greater than that from the 1/8 in. plate welds shown in Figure 1. This is due to the combination of a larger volume of heated material and more efficient geometry for reception of the pulses. The radiograph of the good weld in 304L SS shows no visible defects, but several cracks and voids are apparent in the radiograph of the defective weld in 316 SS. (The weld in 316 SS was caused to crack by the addition of titanium to the weld on the second and fourth weld passes.) The onset of crack formation is evidenced by a sharp increase in acoustic emission shortly after the beginning of the second pass, while emission during the first pass compares favorably with that from the good weld. The sharp increase in acoustic emission at the beginning of the third, fourth, and fifth passes in the defective weld is believed to be caused by the establishment of thermally induced stress gradients in the already defective weldment.

The time delay between originating a defective weld region and the onset of emission varies from approximately 20 sec to 45 sec for the welds shown in Figures 1 and 2. A delay is to be expected since the weldment must at least begin to solidify before stress gradients build up, but the time delay should vary with

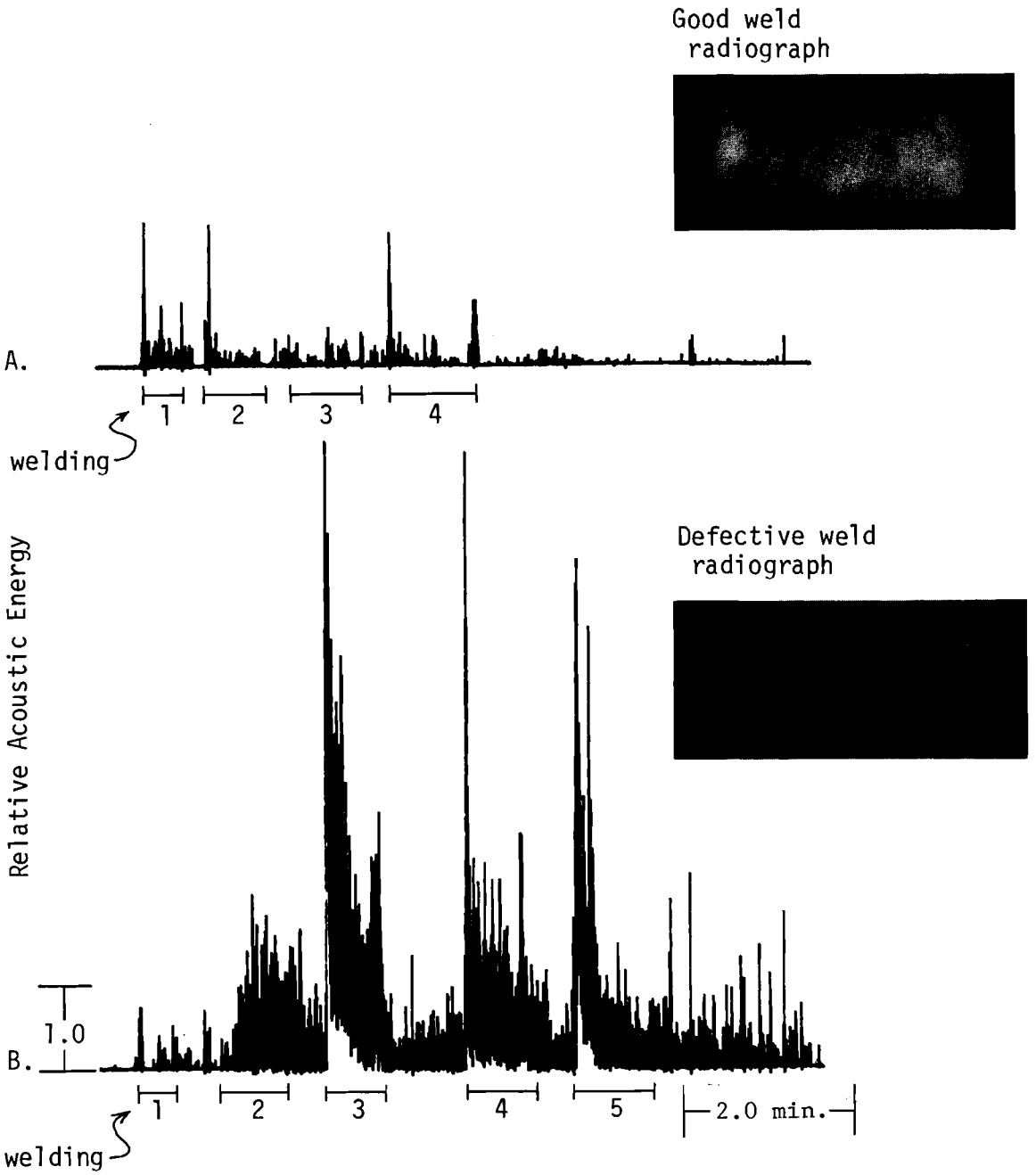

FIGURE 2. *Comparison of Acoustic Emission from a Good Weld (A) and a Defective Weld (B) in 1/2 in. Stainless Steel Plate*

material, cooling rate, and type of defect. Photographs of the completed weld specimens which show the results of radiographic analysis are presented in Figure 3. The 1/8 in. plate welds show marks bracketing the defective regions. A long section of Weld 2 (b_1) is marked for lack of penetration. The acoustic emission data give no evidence of this defect.

ACOUSTIC EMISSION RATE

The acoustic emission signals presented in Figure 1 were originally recorded on magnetic tape with a bandwidth of 300 Hz to 300 kHz to allow further analysis of the data. The tapes were computer processed to generate a running total of acoustic emission pulses and acoustic emission rate as a function of time from the start of the weld. The smoothed acoustic emission rate plots of Figure 4 were obtained using a differential time interval of 1/2 min. Defect markers indicate the time at which the welder passed over the defect region, as in Figure 1.

Smoothing the emission rate plots caused two undesirable effects. The defect in Weld 1 (A) and the second defect in Weld 2 (B) appear to begin emission before being welded over, and the first defect in Weld 3 (C) is lost completely. Reference to Figure 1 shows that the first defect in Weld 3 produced only two intense pulses and four weak pulses in a 2 min period so the emission rate taken at 1/2 min intervals does not exceed the background level.

Acoustic emission rate reached a maximum value within 1 min following welding of the defects and exceeded the background level for 1 to 1 1/2 min. The values are approximate because of the smoothed curves, but they serve to demonstrate that a particular group of emissions can be associated with a particular defect. A weak correlation is noticeable between maximum acoustic emission rate and the number of cracks in a defect region.

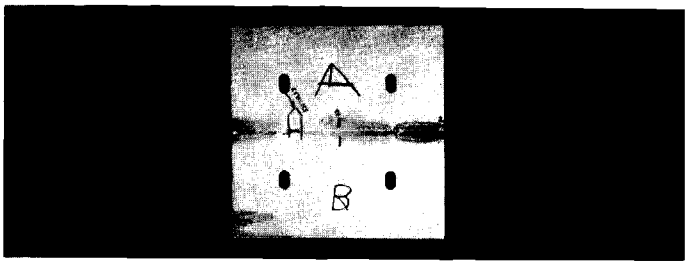

a. Weld 1 - length 12 in. 1/8 in. 304L SS plate

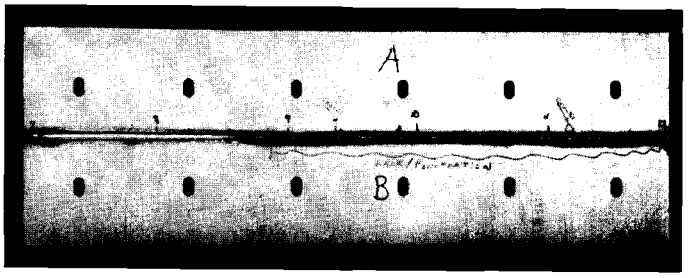

b. Weld 2 - length 36 in. 1/8 in. 304L SS plate

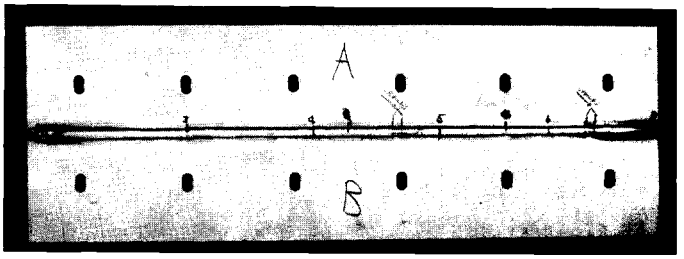

c. Weld 3 - length 36 in. 1/8 in. 304L SS plate

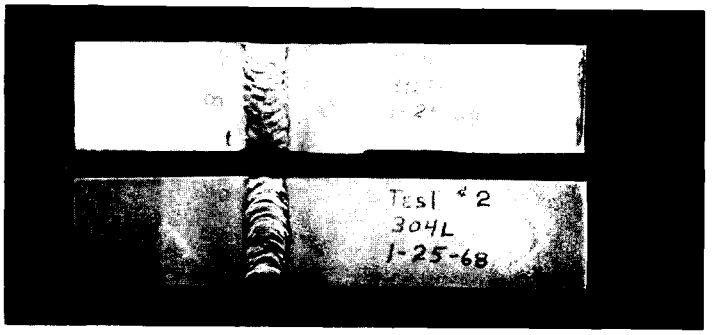

d. Defective Weld - length 2 in. 1/2 in. 316 SS plate

e. Good weld - length 2 in. 1/2 in. 304L SS plate

FIGURE 3. Specimens Used for the Evaluation of Acoustic Emission from Welds

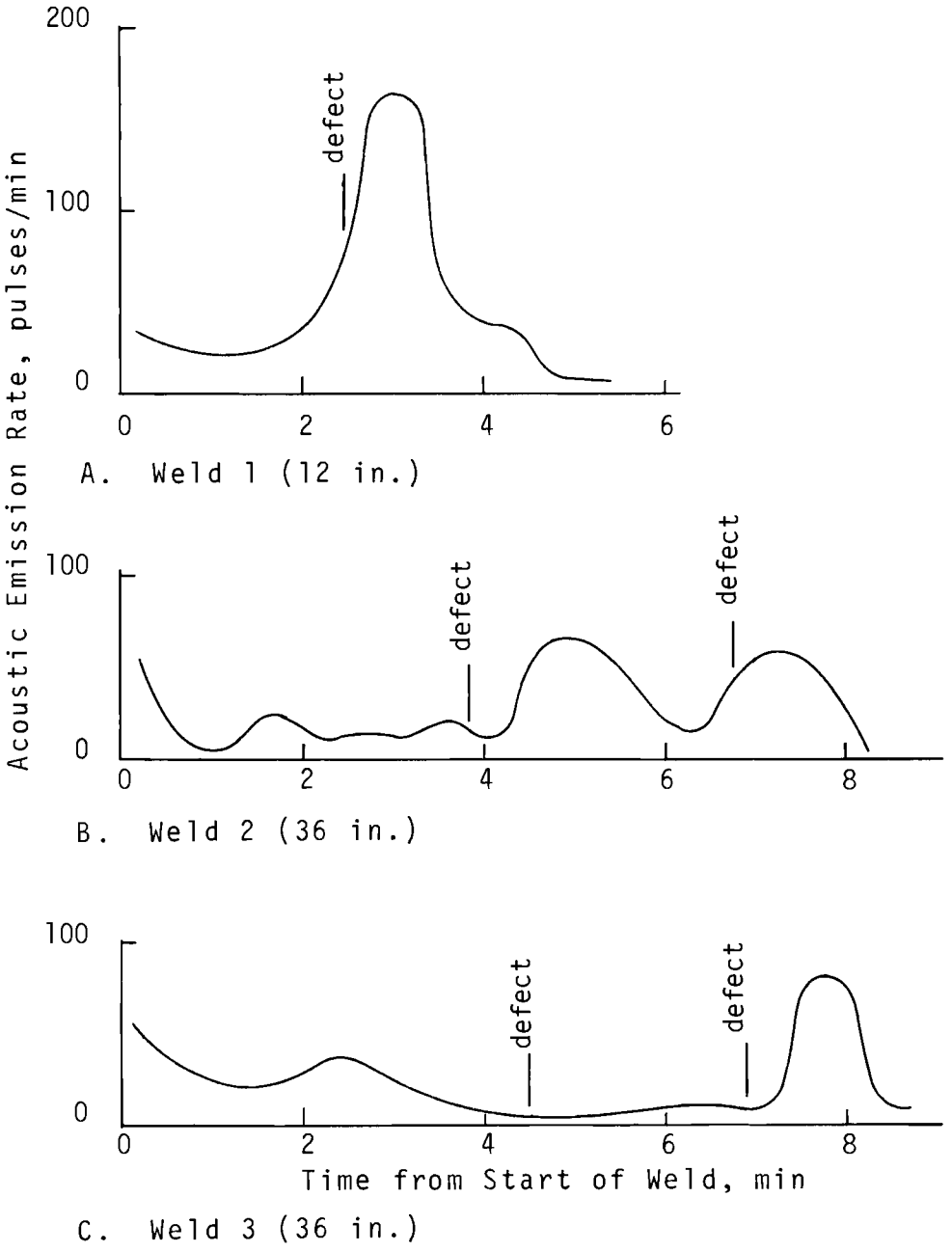

FIGURE 4. Acoustic Emission Rate from Single Pass Welds Relative to Defect Location

The high initial rate of acoustic emission in Welds 2 and 3 was caused by interference from the alternating exciter current which operates until the welding arc is stablized.

TEMPERATURE DEPENDENCE

Thermocouples were mounted beside each weld seam so that, as the welder passed by, the thermocouples would be embedded in the fusion zone. Only two of the thermocouples did embed in the fusion zone. Temperature versus time data were recorded on the magnetic tape along with acoustic emission and welder position. The temperature data obtained from the two thermocouples were averaged and plotted in Figure 5 as a function of time starting as the welder passed over the thermocouple. It should be pointed out that the temperature versus time relationship shown here is approximate and only applies to a particular weld configuration, and to the materials involved.

Based on the assumption that this temperature versus time relationship applies to any point along the weld, a time to temperature conversion was made for each of the defects shown in Figure 4. Data from the four defects, normalized and averaged, are shown in Figure 6. The graph shows that the normalized emission rate reaches a maximum near 400 °C as the defect region cools. This indicates that a major portion of the emission observed is due to hot cracking of the metal in the weldment.[4] This emission rate versus temperature relationship is probably a strong function of the method of inducing defects in the weldment. One would not expect normally occuring defects to exhibit the same emission rate versus temperature relationship as shown here, but the point is made that a relationship does exist between emission rate and weld temperature.

VELOCITY MEASUREMENT

Two acoustic emission receivers were positioned on a line parallel to the weld seam in Weld 3 near the ends of the plate

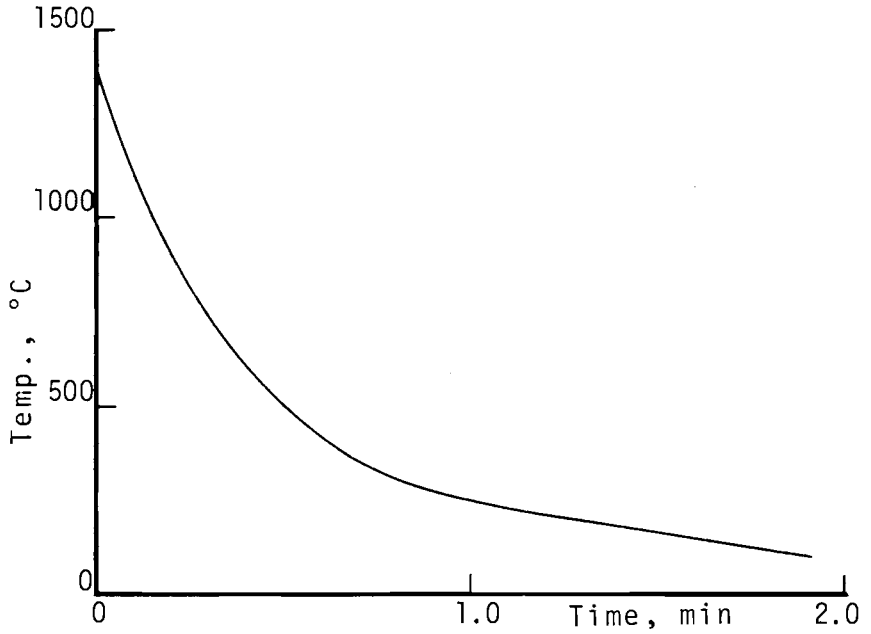

FIGURE 5. Weldment Temperature as a Function of Time from the Molten State

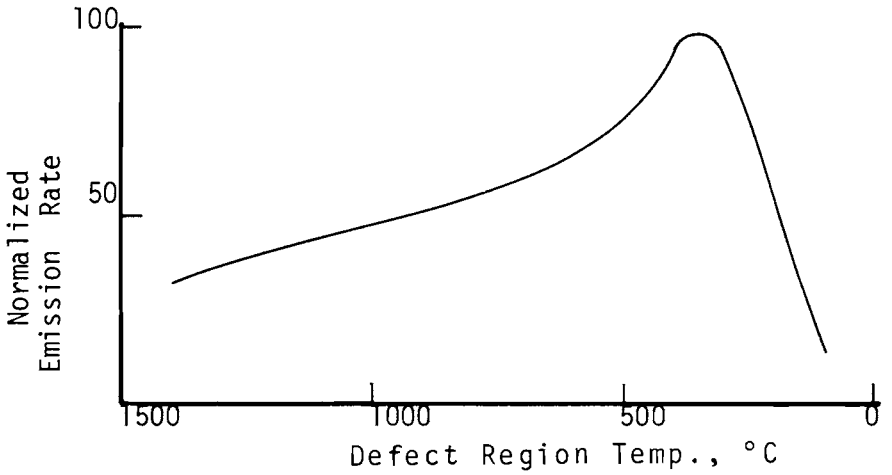

FIGURE 6. Acoustic Emission Rate as a Function of Defect Temperature (Average of 4 Induced Defects)

(Figure 7A) for the purpose of locating individual emission sources in the weld. This was to be accomplished by computing the path difference (d_1-d_2, Figure 7A) from an emission source to the two receivers using the velocity of propagation (v) and the measured difference in time of arrival Δt at the two receivers.

$$(d_1-d_2) = \Delta d_{12} = v\Delta t_{12} \qquad (1)$$

Examples of the measurement of Δt are shown in Figure 7B for pulses from defects F_1 (Δt_{12} = 18 μsec) and F_2 (Δt = 113 μsec) which could be identified by audible cracks recorded on the voice channel of the tape recorder. (Correction for a difference in record to playback head spacing of 17 μsec has been made.) Using these values of Δt and the values of Δd shown in Figure 7B, the apparent velocity of propagation was determined from F_1 and F_2.

$$v_{12} = \frac{\Delta d_{12}}{\Delta t_{12}} = \frac{5.63}{18 \times 10^{-6}} = 3.13 \times 10^5 \text{ in./sec} \qquad (2)$$

$$v_{34} = \frac{\Delta d_{34}}{\Delta t_{34}} = \frac{19.88}{113 \times 10^{-6}} = 1.76 \times 10^5 \text{ in./sec} \quad . \qquad (3)$$

This is surprising since the velocity of propagation of acoustic emission is generally taken to be approximately shear wave velocity[1] which for 304L SS is 1.21×10^5 in./sec.[5]

Five other values of apparent acoustic emission velocity were obtained in a similar manner from Weld 2 and other identifiable pulses from Weld 3. Values of velocity obtained are shown in Table I.

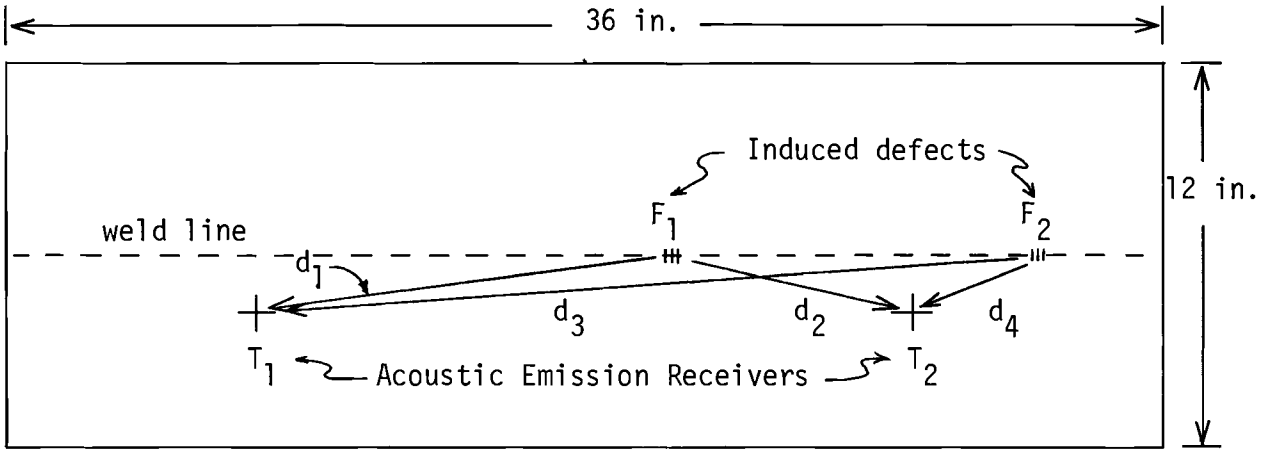

A. Weld Plate 3 Showing Relative Location of Receivers and Defects

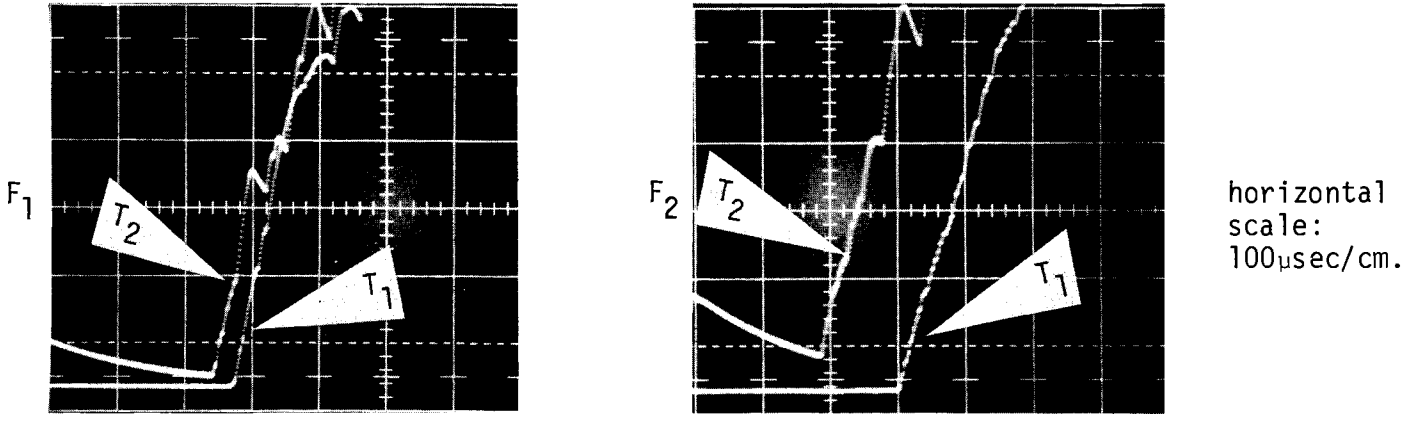

$d_1 - d_2 = 5.63$ in.

$d_3 - d_4 = 19.88$ in.

B. Acoustic Emission Pulses from Induced Defects (rectified)

FIGURE 7. Measurement of Acoustic Emission Velocity

Accurate measurement of difference in time of arrival depends on the ability to identify a feature common to both signals of a signal pair. Figure 8 demonstrates the difficulty encountered: the signal pairs do not exhibit a common feature even at the leading edge.

The difference in received signal characteristics is further demonstrated in the spectral power distribution for a signal pair from a single emission source (Figure 9). The signal received by T_1 has spectral peaks at about 19 kHz and 73 kHz, but the signal at T_2 has spectral peaks at about 11 kHz and 94 kHz. Other acoustic emission pulses exhibited from one to nine spectral peaks ranging from 10 kHz to 270 kHz. The spectral power distribution varies from pulse to pulse and from receiver to receiver in an apparently random manner.

The most plausible explanation of the variation in signal characteristics and velocity with respect to source location and direction is that the received signals are the result of multipath interference at the receiver. The output signal is the instantaneous algebraic sum of the displacement components normal to the plate surface of all acoustic waves simultaneously present at the receiver. Direct longitudinal and shear waves from an emission source a few inches away would excite the receiver only slightly because of the collimation imposed by the 1/8 in. plate. The receivers would be excited primarily by surface waves. The signals received in a bandwidth of 300 Hz to 300 kHz are sustained for up to 10 msec which corresponds to a distance in the plate for surface waves up to 93 ft. Since the acoustic waves radiate in every direction from the emission source, a complicated standing wave pattern gradually builds up in the plate. Since the received signal is the resultant of all the waves which intersect at the receiver location, the received signal characteristics are determined by source location, receiver location, and plate geometry.

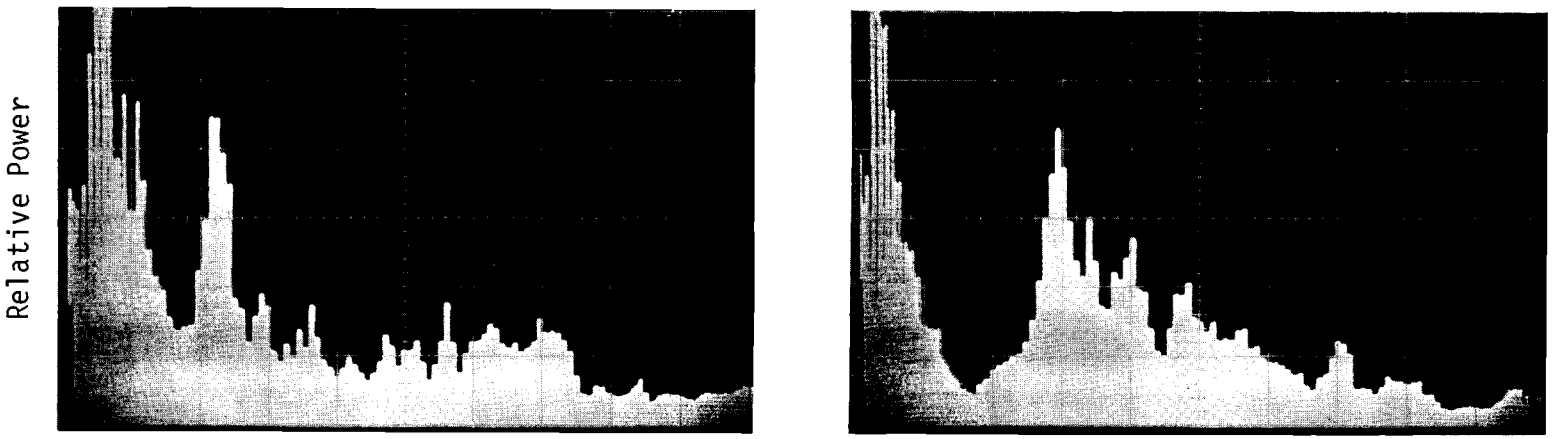

A. Pulse Received by T_1

B. Pulse Received by T_2

FIGURE 9. Spectral Power Distribution from a Single Acoustic Emission Pulse - 1 kHz to 320 kHz

EXPERIMENTAL EQUIPMENT

Acoustic emission and related data, such as weld temperature and welder position, were recorded on magnetic tape for later analysis. A block diagram of the acoustic emission monitoring system is shown in Figure 10. An Ampex 14 channel FR-1300 was used to accommodate three different preamplifier outputs from each of three acoustic emission receivers, two thermocouples, a welder position indicator, and a voice channel. One of the three acoustic emission receivers was not mounted on the weld plate but was used to monitor background noise and power line interference. Preamplifiers with gains of 10^2, 10^3, and 10^4 in a passband of 50 to 300 kHz with 6 dB per octave roll off were connected to each acoustic emission receiver so that emission pulses of both low and high amplitude would be recorded at acceptable levels on the magnetic tape. Signals were recorded at a tape speed of 60 in./sec which results in a record-to-playback transfer function of unity for the direct record-playback modules with a bandwidth of 300 Hz to 300 kHz.

Acoustic emission receivers were 0.240 in. diam PZT-5 units. The receivers were mounted parallel to the weld coupon surface by means of a phenolic support block and acoustically coupled with uncured RTV sealant compound.

Frequency modulation plug-in modules with frequency response from direct current to 20 kHz were used to record and playback the thermocouple outputs and the welder position indicator data.

Acoustic emission data were reproduced directly on an X-Y plotter by rectifying the emission signals. The inertia of the pen drive mechanism integrated the rectified signals to produce the data shown in Figures 1 and 2.

Spectrum analysis of individual pulses was accomplished by re-recording single pulses on short tape loops. The tape loops were then played back into a Tektronix 1L5 Spectrum Analyzer unit to produce the data shown in Figure 9.

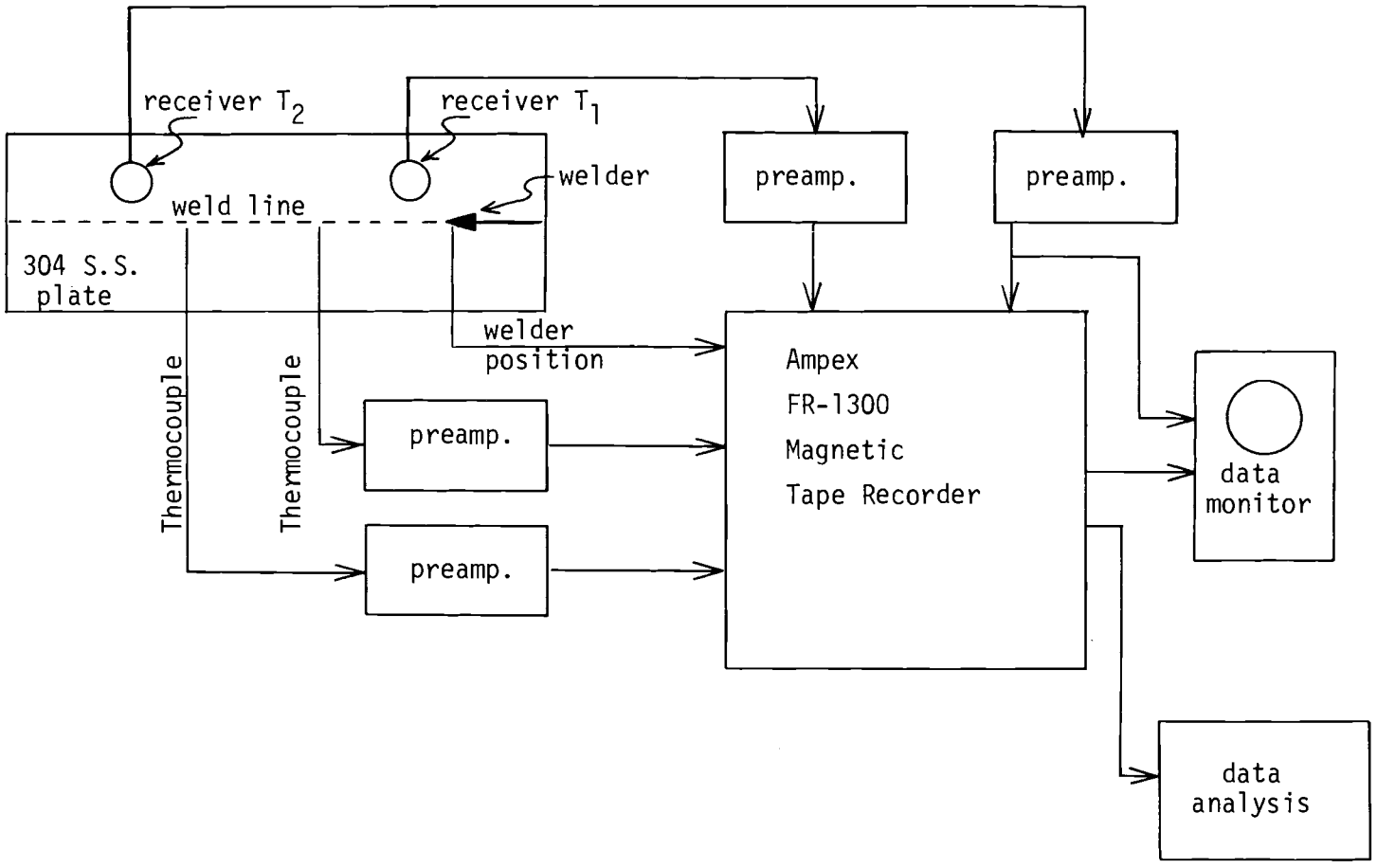

FIGURE 10. Acoustic Emission Monitoring System

ACKNOWLEDGEMENTS

The author expresses appreciation to W. F. Brown for his assistance in the design of the welding fixture and fabrication of the welds used in this investigation.

REFERENCES

1. P. H. Hutton. *Acoustic Emission in Metals as a NDT Tool*, BNWL-SA-1262. Pacific Northwest Laboratory, Richland, Washington. Presented at the 27th National Conference-SNT at Cleveland, Ohio. October 18, 1967.

2. D. L. Parry. *Nondestructive Flaw Detection by Use of Acoustic Emission*, IDO-17230. Phillips Petroleum Company, Idaho Operations Office, Idaho Falls, Idaho. May 1967.

3. C. K. Day. *In-Flight Aircraft Fatigue Detection*. Battelle-Northwest, Richland, Washington, March 1968.

4. A. S. Tetelman and A. J. McEvily, Jr. *Fracture of Structural Materials*. John Wiley & Sons, Inc., New York, N. Y. 1967. p. 542.

5. W. D. Jolly. *Materials Characterization Study*, BNWL-547. Pacific Northwest Laboratory, Richland, Washington, October 1967.

APPENDIX

WELD FABRICATION

APPENDIX

WELD FABRICATION

The following is a detailed description of the equipment and procedures used in the fabrication of the welds used in this investigation.

1. Materials

Base Material - The base material was on ASTM, Type 304 SS plate 1/8 in. thick.

Filler Material - The filler material conformed with ASTM A371-62T, Type 308L specifications.

Electrode - A 2% thoriated tungsten electrode conforming with ASTM B297-65T, Type EWTH-2 specifications was used.

Inert Gas - Welding grade argon of 99.99% minimum purity was used for the shielding gas.

2. Joint Design

The joint design was a butt joint with a single v-groove having a 75 degree included angle. The root face was approximately 1/32 in. The root opening was approximately 3/32 in.

3. Base Material Preparation

Edge Preparation - The plate edges were beveled by machining.

Cleaning - Prior to welding, the plates were degreased with acetone.

4. Welding Process

Welding was accomplished by the automatic gas tungsten-arc process with an automatic filler wire feed.

5. Welding Equipment

The welding equipment was a fully automatic Sciaky Brothers Company welding machine with a 300 A dc rectifier type power supply. The wire feeding mechanism and the torch were

mounted on an automatically controlled movable carriage. In addition to controlling welding current, welding voltage, speed and wire feed, the equipment was programmed to provide a current rise from a low level at the start of the weld to the welding current and to decay the current to a low level at the end of the weld. Gas preflow and postflow was used to purge gas lines and prevent oxidation to the weld metal and tungsten electrode at the end of the weld.

6. Welding Fixture

The plates to be welded were slotted to accommodate 1/2 in. diam hold-down bolts which clamped the plates to a 3/4 x 12 x 36 in., Type 304 SS base plate. A copper backing bar (3/8 x 36 in.), to back up the weld joint, was inserted into the center of the base plate along the longitudinal axis. A small grove 3/16 in. wide by 0.030 to 0.040 in. deep was machined into the center of the copper bar along the 36 in. length.

7. Welding Position

Welding was done in the flat position.

8. Welding Procedure

Welds were made in a single pass.
Shielding gas flow rate was 30 ft^3/min.
Shielding gas nozzle was 5/8 in. diam.
The electrode was 3/32 in. diam. The arc end of the electrode was tapered to approximately 1/32 in. diam.
No purging gas at the back side of the joint was used.
Direct current, straight polarity was used (tungsten electrode negative and work plate positive).
The speed of travel was 4 7/16 in./min.
The filler wire feed speed was 40 in./min as indicated on the wire feeder indicator meter.

The filler wire was 0.035 in. diam.
The arc voltage was 10 V.
The welding current was as follows:
First weld on 12 in. long plate - first 3 in. - 133 A; last 9 in. - 130 A.
Second weld on 36 in. long plate - 125 A.
Third weld on 36 in. long plate - 130 A.

9. Discussion of Results

Since the only filler wire available at the time was 0.035 in. diam, it was used for this study. Although the bead profile was fair, 0.045 diam wire would have produced a more satisfactory surface profile. The plates pulled together toward the end of the weld on the first 36 in. joint and penetration was not entirely satisfactory. On the second 36 in. joint, the current was increased and the hold-down bolts were tightened more than on the previous joint. The additional tightening of the bolts prevented the plates from drawing together. Because the plates did not pull together, the increase in current was not necessary and as a result the weld had the appearance of having a slight amount of excess penetration. If more welds are to be made by this method, attention to the above items should improve the procedure and the results.

Weld coupons for the manual welds shown in Figure 2 (1/2 x 2 x 6 in.) were prepared from 304 and 316 SS. The coupons were beveled along the 2 in. dimension to form a 75 degree included angle at the weld seam. The welds were made by the GTA process using 308 SS filler metal. In addition, short pieces of titanium rod were laid in the weld trough prior to the second and fourth weld passes and melted into the weld in 316 SS in order to produce defects in that weld. The coupons were clamped to a 1/2 in. thick steel plate to prevent warpage during the weld.

DISTRIBUTION

No. of Copies

OFFSITE

2 AEC Chicago Patent Group
- G. H. Lee

3 AEC Division of Isotope Development
- W. K. Eister
- G. Y. Jordy
- J. N. Maddox

8 AEC Division of Reactor Development and Technology
- J. F. Dobson
- J. S. Griffo
- K. E. Horton
- W. K. Kern
- J. A. Lieberman
- J. A. Powers
- S. J. Seiken
- J. M. Simmons

238 AEC Division of Technical Information Extension

1 Aerojet General Nucleonics
- W. G. Ruehle

1 Brookhaven National Laboratory
- J. H. Cusack

2 Hittman Associates, Inc.
4715 Wabash Avenue E.
Baltimore, Maryland 21215
- F. D. Altieri
- D. E. Goslee

2 Minnesota Mining and Manufacturing Company
- V. Yanisch
- R. L. Panneman

2 Monsanto Research Corporation (AEC)
- C. M. Henderson
- P. L. Johnson

No. of Copies

1 Oak Ridge National Laboratory
R. R. Robinson

1 Westinghouse Electric Corporation (AEC)
S. Cerni

ONSITE-HANFORD

1 AEC Chicago Patent Group
R. K. Sharp (Richland)

2 AEC RDT Site Representative-PNL
P. G. Holsted

1 AEC Richland Operations Office
C. L. Robinson

2 Atlantic Richfield Hanford Company
W. P. McCue

3 Battelle Memorial Institute

2 Douglas United Nuclear Inc.
Files

49 Battelle-Northwest

W. F. Brown
G. M. Dalen
C. K. Day
C. J. Denton
G. E. Driver
R. J. Hoch
P. H. Hutton
R. N. Johnson
W. D. Jolly (25)
R. N. Ord
H. N. Pedersen
J. C. Spanner
W. G. Spear
R. W. Steffens
C. D. Swanson
J. C. Tobin
E. E. Voiland
D. C. Worlton
Technical Files (5)
Technical Publications (2)